



## An acyclic aluminyl anion†

 Cite this: *Chem. Commun.*, 2023, 59, 5277

 Ross A. Jackson,‡<sup>a</sup> Aidan J. R. Matthews, <sup>b</sup> Petra Vasko, <sup>c</sup> Mary F. Mahon,<sup>a</sup> Jamie Hicks <sup>\*b</sup> and David J. Liptrot <sup>\*a</sup>

 Received 16th March 2023,  
 Accepted 6th April 2023

DOI: 10.1039/d3cc01317k

rsc.li/chemcomm

The potassium aluminyl complex  $K_2[Al(N(Dipp)SiMe_3)_2]_2$  was synthesised *via* reduction of  $[Al(N(Dipp)SiMe_3)_2]$  (Dipp = 2,6-*i*-Pr<sub>2</sub>C<sub>6</sub>H<sub>3</sub>). This represents the first example of an aluminyl anion supported by an acyclic ligand framework. Attempts to yield the same structure with a larger ligand framework,  $\{N(Dipp)Si(i-Pr)_3\}$ , led to C–H cleavage.  $K_2[Al(N(Dipp)SiMe_3)_2]_2$  behaves as a nucleophilic source of aluminium; reaction with an electrophilic  $\beta$ -diketiminato supported magnesium(II) iodide forms a monomeric, acyclic magnesium aluminyl complex.

Since the pioneering report by Goicoechea, Aldridge and co-workers in 2018,<sup>1</sup> the synthesis, structure, and reactivity of aluminyl anions (a.k.a. alumanyl anions) continues to be hot topic in organometallic chemistry.<sup>2</sup> This is due both to fundamental interest, and also due to these nucleophilic anions allowing access to various aluminium-containing compounds that have been inaccessible *via* traditional routes.<sup>2,3</sup> Aluminyl anions are highly reactive species that are isoelectronic to carbenes when charge separated from their counterion.<sup>2</sup> This electronic structure opens the possibility of ambiphilic reactivity as the aluminium centre possesses both a lone pair of electrons and an empty p-orbital, but recent reports have been dominated by their reactivity as aluminium-centred nucleophiles.<sup>1–4</sup> This is in stark contrast to the reactivity typically associated with aluminium compounds (*i.e.* electrophilicity).<sup>5</sup>

The library of reported aluminyl anions has expanded rapidly over the last few years, with the interactions between the anions and their corresponding cations playing an important role in the

structure and reactivity of these compounds.<sup>2,5</sup> The ligands used to stabilise these aluminyl anions are also critical to their structure and reactivity. Slight variations in the donor atoms and angles have been shown to dramatically impact the frontier orbitals of the anions and consequently their reactivity.<sup>2</sup> As can be seen in Fig. 1, a range of ligands have been used to stabilise ‘free’ aluminyl anions, *i.e.*, those containing little or no covalent interaction between the Al centre and their cation. The first reported aluminyl anion by Goicoechea and Aldridge (**I**) was stabilised using a large, chelating, xanthene-based diamido ligand.<sup>1</sup> This was followed by the groups of Coles, Hill and McMullen, Harder, and Yamashita, who have since used a series of bidentate diamido ligands to isolate a series of 6- and 7-membered aluminyl anions (**II–V**).<sup>6–11</sup> The groups of Kinjo and Yamashita have recently contributed a series of 5-membered aluminyl anions, stabilised by bidentate alkyl(amido) (**VI–VII**) and dialkyl (**VIII**) ligands.<sup>12–14</sup>

Even though the range of ligands used to isolate ‘free’ aluminyl anions appears to be diverse, to date all of these are dianionic chelating ligands.<sup>1,6–14</sup> This is in fact the case for

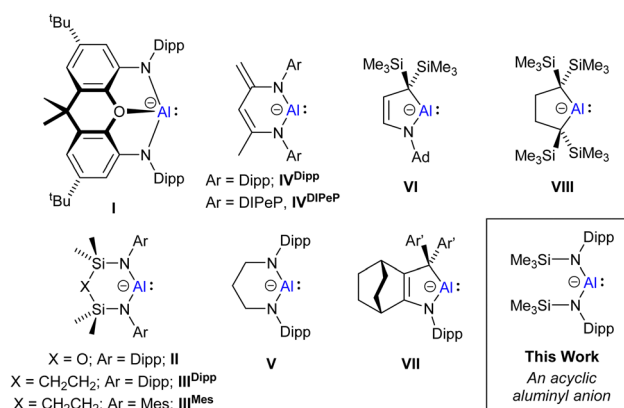


**Fig. 1** Previously reported cyclic aluminyl anions (**I–VIII**) and the first acyclic aluminyl anion reported in this work. Cations excluded for clarity. Dipp = 2,6-*i*-Pr<sub>2</sub>-phenyl, DIPEP = 2,6-C(H)Et<sub>2</sub>-phenyl, Ar' = 3,5-*t*-Bu-phenyl.

<sup>a</sup> Department of Chemistry, University of Bath, Bath, BA2 7AY, UK.

E-mail: d.j.liptrot@bath.ac.uk

<sup>b</sup> Research School of Chemistry, Australian National University, Acton, ACT, 2601, Australia. E-mail: jamie.hicks@anu.edu.au

<sup>c</sup> Department of Chemistry, University of Helsinki, A.I. Virtasen aukio 1, P.O. Box 55, FI-00014, Finland

 † Electronic supplementary information (ESI) available: Full experimental and computational details, characterisation data. CCDC 2218546–2218550. For ESI and crystallographic data in CIF or other electronic format see DOI: <https://doi.org/10.1039/d3cc01317k>

‡ Equal contribution.



nearly all reported group 13 E(I) anions (boryl, aluminyl, gallyl, indyl), with no mononuclear acyclic boryl, aluminyl or indyl anions bearing *s*-block cations being reported.<sup>15,16</sup> Herein, we report the first acyclic aluminyl anion, stabilised by two bulky monodentate, monoanionic amido ligands and explore its structure and reactivity.

Two acyclic, bisamido aluminium iodide complexes,  $[Al\{N(\text{Dipp})SiR_3\}_2]$  ( $R = i\text{-Pr}$ , **1**;  $\text{Me}$ , **2**), were synthesised as potential precursor complexes to acyclic aluminyl anions. These precursors were initially targeted through salt metathesis reactions between two equivalents of the respective alkali metal ligand salt and aluminium(III) iodide. Whilst this furnished **1** in good yield, repeated attempts to synthesise **2** through this route provided intractable materials and inconsistent results. Instead, **2** was synthesised by a route inspired by Stalke and Heine's report of  $[LiAlH_2\{N(\text{SiMe}_3)_2\}_2]$ ;<sup>17</sup> two equivalents of  $\text{HN}(\text{Dipp})\text{SiMe}_3$  were refluxed with lithium aluminium hydride in diethyl ether for 6 days. Treatment of the resultant solution with excess trimethylsilyl iodide followed by sublimation furnished **2** in moderate yields. Both compounds **1** and **2** were recrystallised and subjected to analysis by SC-XRD (see ESI†).

With the desired iodides in hand, we turned our attention to reduction hoping to access the corresponding acyclic aluminyl anions (Scheme 1). Reaction of **1** with excess  $\text{KC}_8$  or 5% w/w  $\text{K/KI}$ <sup>18</sup> initially seemed promising, resulting in orange-coloured solutions as had previously been described in the synthesis of other aluminyl anions.<sup>1,6–14</sup> However, these solutions rapidly lost colour at room temperature, suggesting onward reactivity of any such species present. Crystallisation of the resultant solution from a  $\text{K/KI}$  reduction furnished material suitable for single crystal X-ray crystallography (compound **3**, Fig. 2).

Compound **3** is a potassium aluminate where the coordination sphere of the aluminium contains one hydride and one equivalent of the  $[N(\text{Dipp})\text{Si}(i\text{-Pr})_3]^-$  ligand. Alongside this, it contains a bidentate, dianionic ligand  $[N(\text{Dipp})\{\text{Si}(i\text{-Pr})_2\text{CMe}_2\}]^{2-}$  derived from a C–H cleavage of the tri-*iso*-propylsilyl substituent of the ligand. The potassium counterion is closely associated with the hydride and arene substituents of both the  $[N(\text{Dipp})\text{Si}(i\text{-Pr})_3]^-$  and

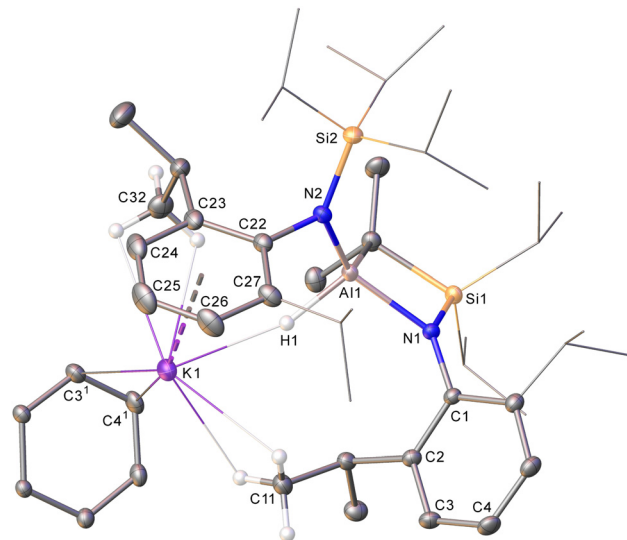


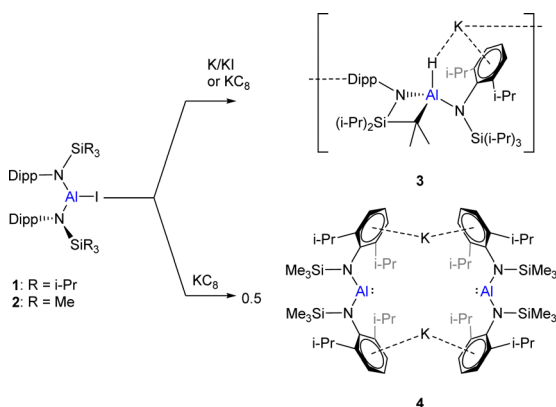
Fig. 2 Molecular structure (30% probability ellipsoids) of  $\text{K}\{[Al\{N(\text{Dipp})\text{Si}(i\text{-Pr})_2\text{CMe}_2\}]_2\}^-$  (**3**). Most hydrogen atoms have been omitted for clarity. *iso*-Propyl groups without interactions to the potassium centres have been represented in wireframe view, also for visual ease. Symmetry operations for labels with superscripts: <sup>1</sup> $1-x, -\frac{1}{2}+y, \frac{1}{2}-z$ ; <sup>2</sup> $1-x, \frac{1}{2}+y, \frac{1}{2}-z$ .

$[N(\text{Dipp})\{\text{Si}(i\text{-Pr})_2\text{CMe}_2\}]^{2-}$  ligands giving rise to a coordination polymer through  $\text{K} \cdots \text{arene}$  interactions in the solid state.

Compound **3** is proposed to have been produced *via* reduction of the corresponding iodide to a lower oxidation state aluminium compound which then proceeds towards ligand activation. Whilst this may be *via* formation of the desired acyclic aluminyl anion  $\text{K}_n[Al\{N(\text{Dipp})\text{Si}(i\text{-Pr})_3\}_2]_n$ , which then undergoes an intramolecular oxidative addition of a ligand C–H bond, radical pathways cannot be ruled out. Nevertheless, aluminyl anions have previously been shown to oxidatively add a range of C–H bonds.<sup>2</sup>

In contrast, addition of an excess of  $\text{KC}_8$  to compound **2** in benzene provided a bright yellow solution, which persisted indefinitely under an inert atmosphere. Crystallisation of this solution provided X-ray quality crystals of the acyclic potassium aluminyl anion  $\text{K}_2[Al\{N(\text{Dipp})\text{SiMe}_3\}_2]^-$  **4** (Fig. 3).

Compound **4** crystallises as a dimer comprising a pair of  $[Al\{N(\text{Dipp})\text{SiMe}_3\}_2]^-$  anions with bridging potassium cations coordinated in an  $\eta^6$ -fashion to the arene substituents on the ligand. This structure is analogous to a number of the reported cyclic potassium aluminyl complexes.<sup>1,6–11</sup> However, compound **4** represents the first structurally characterised acyclic aluminyl anion. It is related to  $\text{K}_2[\text{III}^{\text{Dipp}}]_2$  *via* a conceptual C–C cleavage of its ligand backbone. The enhanced steric demand of two  $[N(\text{Dipp})\text{SiMe}_3]^-$  ligands *versus* the bidentate diamide in  $\text{K}_2[\text{III}^{\text{Dipp}}]_2$  results in a widening of the Al–N–Si angles (**4**, range 135.5(2)–138.6(2);  $\text{K}_2[\text{III}^{\text{Dipp}}]_2$  range 132.06(12)–134.70(12)<sup>7</sup>) and a staggering of the silyl methyl groups in **4**. The absence of chelation in **4** results in a significant deviation in its N–Al–N angle (**4**, 116.33(16), 116.61(17);  $\text{K}_2[\text{III}^{\text{Dipp}}]_2$ , 108.84(9), 108.77(9)) and Al···Al distances compared to  $\text{K}_2[\text{III}^{\text{Dipp}}]_2$  (**4**, 6.014(3), 6.047(3);  $\text{K}_2[\text{III}^{\text{Dipp}}]_2$  5.271(1) Å). The Al···K distances,



Scheme 1 The results of reducing compounds **1** and **2** to generate compounds **3** and **4**.



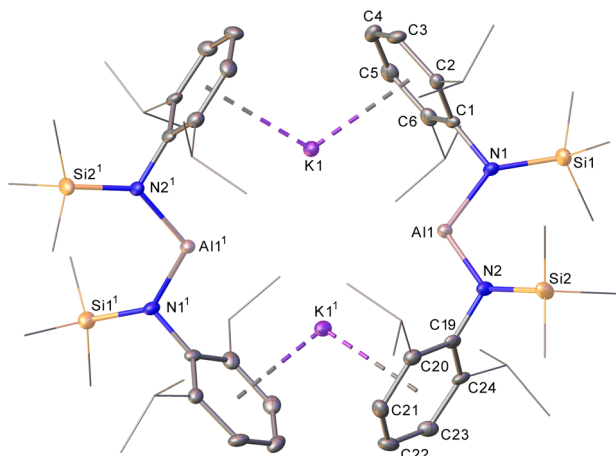


Fig. 3 Molecular structure (30% probability ellipsoids) of  $K_2[Al\{N(Dipp)SiMe_3\}_2]$  (**4**). Hydrogen atoms have been omitted and both iso-propyl and methyl groups have been represented in wireframe format, for clarity. Symmetry operations for labels with superscripts:  $^11-x, 1-y, -z$ .

in contrast, are similar (**4**, range 3.5995(16)–3.7380(16);  $K_2[III^{Dipp}]_2$  range 3.584(1)–3.625(1) Å). The conservation of such distances reiterates that these interactions with the potassium counterions assist in the generation of isolable, dimeric donor-free aluminyl anion systems.

$^1H$  DOSY NMR was acquired to analyse the solution state structure of compound **4**. The diffusion coefficient for **4** was determined to be  $5.87 \times 10^{-10} m^2 s^{-1}$ , which converts into a hydrodynamic radius of 6.74 Å. This value closely matches the radius calculated from the dimeric solid-state structure (6.42 Å) and is in line with that measured for the related dimeric potassium aluminyl system  $K_2[III^{Dipp}]_2$  (6.55 Å) suggesting **4** is dimeric in solution.

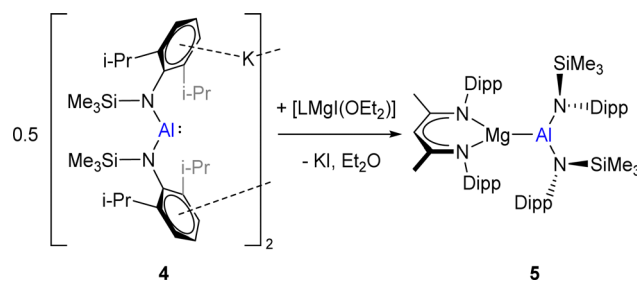
We initially postulated that the increased steric demand of the  $[N(Dipp)Si(i-Pr)_3]^-$  ligand may lead to a wider N–Al–N angle in the corresponding aluminyl anion compared to its trimethylsilyl analogue, with corresponding effects on its reactivity. Thus, we investigated the electronic structures of the targeted and observed aluminyl anions  $[Al\{N(Dipp)Si(i-Pr)_3\}_2]^-$  and  $[Al\{N(Dipp)SiMe_3\}_2]^-$  respectively, by DFT methods. Interestingly, no significant divergence in their stability was reflected in their electronic structures. Similar orbital energies and energy gaps between the lone pair at aluminium (in both cases the HOMO) and an orbital with significant Al  $p_z$  character (LUMO for both; HOMO–LUMO gap for  $[Al\{N(Dipp)Si(i-Pr)_3\}_2]^- = 3.36$  eV; and for  $[Al\{N(Dipp)SiMe_3\}_2]^- = 3.47$  eV) (see ESI† for further details) were calculated. The slightly smaller HOMO–LUMO gap for  $[Al\{N(Dipp)Si(i-Pr)_3\}_2]^-$  could give rise to the instability of the anion and the observed ligand activation chemistry. Indeed, the calculated energy gap between the Al-centred frontier orbitals (the Al lone pair and empty  $p$ -orbital) for  $[Al\{N(Dipp)Si(i-Pr)_3\}_2]^-$  is the smallest in the series of previously calculated monomeric aluminyl anions (ranging from 3.42 to 4.06 eV).<sup>2b</sup> Correspondingly, inspection of the optimised structures for these species reveal a wider N–Al–N angle for  $[Al\{N(Dipp)Si(i-Pr)_3\}_2]^-$  ( $123.23^\circ$ ) than for  $[Al\{N(Dipp)SiMe_3\}_2]^-$

( $111.26^\circ$ , avg.  $116.47^\circ$  in **4**). Alongside these factors, a larger number of C–H  $\cdots M$  interactions are present in  $[Al\{N(Dipp)Si(i-Pr)_3\}_2]^-$  than in  $[Al\{N(Dipp)SiMe_3\}_2]^-$ , potentially predisposing this system to C–H cleavage.

Addition of [2.2.2]cryptand to compound **4** resulted in a deep orange-red solution (similar to that reported for the monomeric potassium aluminyl system  $[K\{[2.2.2]cryptand\}][I]$ ).<sup>19</sup> However, this colour rapidly faded at room temperature and the reaction precipitated intractable, colourless material, resulting in a  $^1H$  NMR spectrum where only [2.2.2]cryptand could be assigned. In addition, thermolysis of **4** led to complex  $^1H$  NMR spectra reflecting a number of products which could not be readily characterised (see ESI†).

Cyclic aluminyl anions are prominent for their reactivity as nucleophilic sources of aluminium,<sup>2</sup> therefore, we were interested to investigate whether the acyclic aluminyl anion **4** maintained this trait. Addition of a  $d_8$ -toluene solution of **4** to the magnesium(II) electrophile  $[(^{Dipp}nacnac)Mg\{I(OEt_2)\}]$  ( $^{Dipp}nacnac = \{[(Dipp)NC(CH_3)_2CH]\}$ )<sup>20</sup> resulted, after 2 days at  $40^\circ C$ , in a loss of the colour associated with compound **4** and a  $^1H$  NMR spectrum consistent with the formation of one major new  $^{Dipp}nacnac$  containing species (Scheme 2). Crystallisation of this reaction mixture gave material appropriate for single crystal X-ray crystallography, showing the product to be  $[(^{Dipp}nacnac)MgAl\{N(Dipp)SiMe_3\}_2]$ , compound **5** (Scheme 2 and Fig. 4).

Compound **5** represents a monomeric acyclic aluminyl anion complex bearing a formal magnesium–aluminium bond. Both the aluminium and magnesium centres are three-coordinate and trigonal planar, with their corresponding planes essentially perpendicular to each other (interplanar angle,  $94.43(4)^\circ$ ), presumably to minimise steric clashes between the ligands. The Al–Mg bond length of 2.7888(6) Å agrees with Al–Mg bond lengths of reported magnesium aluminyl species with bidentate ligands at aluminium, e.g.  $[(^{Mes}nacnac)Mg\{I\}]$  (2.696(1) Å),<sup>1</sup>  $[(^{Mes}nacnac)Mg\{II\}]$  (2.7711(6) Å)<sup>21</sup> and  $[(^{Dipp}nacnac)Mg\{III\}]$  (2.7980(6) Å).<sup>7</sup> The N–Al–N bond angle ( $118.76(5)^\circ$ ) is larger than in its bidentate aluminium ligand analogue  $[(^{Dipp}nacnac)Mg\{III\}]$  ( $111.87(6)^\circ$ )<sup>7</sup> and also slightly larger than that in the starting potassium aluminyl **4** ( $116.33(16), 116.61(17)^\circ$ ). Interestingly, the Dipp groups of the two monodentate amido ligands orient to opposite sides of the Al centre, presumably to minimise steric clashes. This arrangement



Scheme 2 The synthesis of compound **5** from **4** and  $[(^{Dipp}nacnac)Mg\{I(OEt_2)\}]$ .



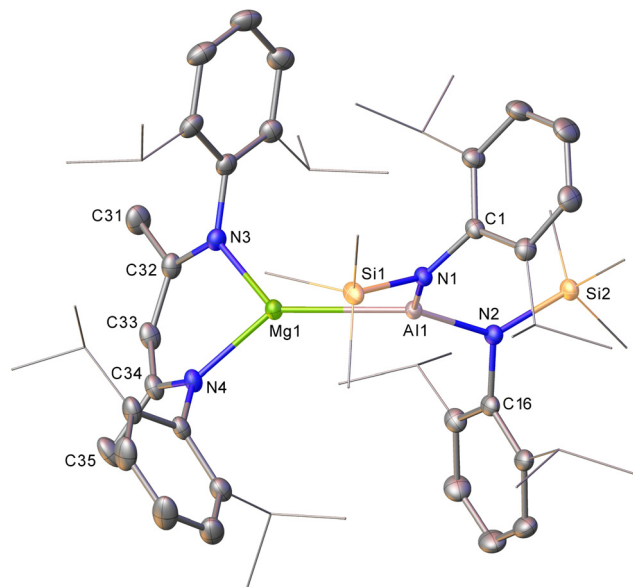


Fig. 4 Molecular structure (30% probability ellipsoids) of one of the molecules in the asymmetric unit of **5**. Solvent and hydrogen atoms have been omitted while iso-propyl groups and silicon bound methyl substituents have been represented in wireframe format, for visual ease.

is not possible in the systems with bidentate ligands at aluminium hitherto described.

Compound **5** was additionally analysed by DFT analysis. The electronic structure of **5** indicates that it is similar to previously reported nacnac magnesium aluminyls.<sup>1,7</sup> This is reflected in the calculated NBO charges for compound **5** (Mg +1.57, Al +0.88) and the BCP as elucidated by QTAIM for the Mg–Al bond ( $\rho(r)$ : 0.033 a.u.,  $\nabla^2\rho(r)$  = 0.038 e  $\text{\AA}^{-5}$  and  $\epsilon$  = 0.021). The covalency in the Mg–Al interaction alongside the significant steric bulk of the ancillary ligand at magnesium most likely precludes activation of the ligand, allowing the isolation of a monomeric, acyclic magnesium aluminyl.

In summary, the first acyclic aluminyl anion has been reported as both a potassium-bridged dimer (**4**) and a monomeric magnesium complex (**5**).

DJL thanks the Royal Society for the support of a University Research Fellowship. JH would like to thank the Australian Research Council (DE190100524 and DP210100454) for the funding of this work. PV would like to thank the Academy of Finland for funding (grant numbers 346565 and 338271), the Finnish Computing Competence Infrastructure (FCCI) and the CSC – IT Center for Science, Finland, for computational resources.

## Conflicts of interest

There are no conflicts to declare.

## Notes and references

- J. Hicks, P. Vasko, J. M. Goicoechea and S. Aldridge, *Nature*, 2018, **557**, 92–95.
- (a) K. Hobson, C. J. Carmalt and C. Bakewell, *Chem. Sci.*, 2020, **11**, 6942–6956; (b) J. Hicks, P. Vasko, J. M. Goicoechea and S. Aldridge, *Angew. Chem., Int. Ed.*, 2021, **60**, 1702–1713; (c) M. P. Coles and M. J. Evans, *Chem. Commun.*, 2023, **59**, 503–519.
- See for example: (a) M. D. Anker, R. J. Schwamm and M. P. Coles, *Chem. Commun.*, 2020, **56**, 2288–2291; (b) M. D. Anker and M. P. Coles, *Angew. Chem., Int. Ed.*, 2019, 18261–18265; (c) J. Hicks, P. Vasko, J. M. Goicoechea and S. Aldridge, *J. Am. Chem. Soc.*, 2019, **141**, 11000–11003.
- See for example: (a) H.-Y. Liu, S. E. Neale, M. S. Hill, M. F. Mahon and C. L. McMullin, *Dalton Trans.*, 2022, **51**, 3913–3924; (b) S. Kurumada and M. Yamashita, *J. Am. Chem. Soc.*, 2022, **144**(10), 4327–4332; (c) J. Hicks, A. Mansikkamäki, P. Vasko, J. M. Goicoechea and S. Aldridge, *Nat. Chem.*, 2019, **11**, 237–241.
- (a) T. X. Gentner, M. J. Evans, A. R. Kennedy, S. E. Neale, C. L. McMullin, M. P. Coles and R. E. Mulvey, *Chem. Commun.*, 2022, **58**, 1390–1393; (b) S. Grams, J. Mai, J. Langer and S. Harder, *Dalton Trans.*, 2022, **51**, 12476–12483.
- R. J. Schwamm, M. D. Anker, M. Lein and M. P. Coles, *Angew. Chem., Int. Ed.*, 2019, **58**, 1489–1493.
- R. J. Schwamm, M. P. Coles, M. S. Hill, M. F. Mahon, C. L. McMullin, N. A. Rajabi and A. S. S. Wilson, *Angew. Chem., Int. Ed.*, 2020, **59**, 3928–3932.
- R. J. Schwamm, M. S. Hill, H.-Y. Liu, M. F. Mahon, C. L. McMullin and N. A. Rajabi, *Chem. – Eur. J.*, 2021, **27**, 14971–14980.
- S. Grams, J. Eysel, J. Langer, C. Färber and S. Harder, *Angew. Chem., Int. Ed.*, 2020, **59**, 15982–15986.
- S. Grams, J. Mai, J. Langer and S. Harder, *Organometallics*, 2022, **41**, 2862–2867.
- K. Koshino and R. Kinjo, *J. Am. Chem. Soc.*, 2020, **142**, 9057–9062.
- G. Feng, K. L. Chan, Z. Lin and M. Yamashita, *J. Am. Chem. Soc.*, 2022, **144**, 22662–22668.
- C. Yan and R. Kinjo, *Angew. Chem., Int. Ed.*, 2022, **61**, e202211800.
- S. Kurumada, S. Takamori and M. Yamashita, *Nat. Chem.*, 2020, **12**, 36–39.
- Two acyclic low oxidation state gallium anions have been reported, although both feature Ga–Ga bonds, see: (a) N. Wiberg, T. Blank, K. Amelunxen, H. Noth, J. Knizek, T. Haberer, W. Kaim and M. Wanner, *Eur. J. Inorg. Chem.*, 2001, 1719–1727; (b) G. Linti, A. Rodig and W. Kostler, *Z. Anorg. Allg. Chem.*, 2001, **627**, 1465–1476.
- An acyclic diborane(4) dianion, which can be considered as a diarylboryl anion equivalent has also been reported: S. Akiyama, K. Yamada and M. Yamashita, *Angew. Chem., Int. Ed.*, 2019, **58**, 11806–11810.
- A. Heine and D. Stalke, *Angew. Chem., Int. Ed. Engl.*, 1992, **31**, 854–855.
- J. Hicks, M. Juckel, A. Paparo, D. Dange and C. Jones, *Organometallics*, 2018, **37**, 4810–4813.
- J. Hicks, P. Vasko, J. M. Goicoechea and S. Aldridge, *J. Am. Chem. Soc.*, 2019, **141**, 11000–11003.
- J. Prust, K. Most, I. Müller, E. Alexopoulos, A. Stasch, I. Uson and H. W. Roesky, *Z. Anorg. Allg. Chem.*, 2001, **627**, 2032–2037.
- M. J. Evans, G. H. Iliffe, S. E. Neale, C. M. McMullin, J. R. Fulton, M. D. Anker and M. P. Coles, *Chem. Commun.*, 2022, **58**, 10091–10094.

